Determination of adsorption isotherms in 3D cylindrical porous media

JOZEF KAČUR
Slovak University of Technology
Department of Physics
Radlinského 11, 810 05 Bratislava
SLOVAKIA
Jozef.Kacur@fmph.uniba.sk

PATRIK MIHALA
Comenius University
Department of MANM
Mlynská dolina, 842 48 Bratislava
SLOVAKIA
pmihala@gmail.com

Abstract: We discuss the numerical modelling of contaminant transport in unsaturated porous media in 3D. The mathematical model represents water mass balance and conservation of contaminant, which is expressed by coupled non-linear system of parabolic-elliptic equations. Mathematical model for water transport in unsaturated porous media is represented by Richard?s type equation. Also diffusion of contaminant in matrix could be included.
The adsorption isotherms are generally non-linear, containing the tuning parameters underlying to determination. We determine these parameters by the methods of inverse problems. A successful experiment scenario is suggested to determine the required parameters. Used complex model in 3D requires also determination of dispersion coefficients. This problem together with suitable experiment scenario is discussed too. The obtained experiments support our method.
We have discussed the adsorption problem in 1D model before, but preferential streamlines in 1D thin tubes shadow accurate results in determination of required parameters.

Key–Words: contaminant transport, adsorption isotherms, unsaturated flow, inverse problems

1 Introduction

We are focused to the the numerical modelling of infiltration of contaminated water into unsaturated porous media and determination of adsorption isotherms. A coupled system with contaminant transport, dispersion and adsorption is considered.

The main contribution is focused to the determination of adsorption isotherms parameters. The developed numerical method is a good candidate to solve corresponding inverse problems. Numerical experiments support our method.

The mathematical model for unsaturated flow is based on the Richard's non-linear and degenerate equation. The model of contaminant transport is based on the Fick's law and the mass balance equation. Non-linear adsorption is represented by adsorption isotherms and kinetic rates. A correct numerical method is constructed in 3D which can be a good candidate for the solution of inverse problems to determine model parameters in the adsorption part of the model. Our numerical method is based on flexible time stepping and operator splitting by means of which we decompose the complex strongly non-linear system to its natural parts: flow in unsaturated porous media, transport with diffusion and dispersion of contaminant and its adsorption.

Our previously developed numerical model for 1D suffers in practical laboratory experiments from preferential streamlines appearing, specially, when applying centrifugation. Experiments with 3D (cylindrical samples) yield much more of scenarios by means of which we reduce the creation of preferential streamlines.

In series of numerical experiments we demonstrate the effectiveness of our method and suitable experimental scenarios enabling relatively simple measurements used in solution of inverse problems.

2 Mathematical Model

2.1 Water Flow

Our sample is a cylinder with radius R and height Z. We will consider radial symmetrical boundary conditions, therefore we transform the mathematical model using cylindrical coordinates (r, z). Then the governing partial differential equation for infiltration (in gravitational mode) reads as follows

$$\partial_t \theta(h) = \frac{1}{r}\partial_r(rK(h)\partial_r h) + \partial_z(K(h)(\partial_z h - 1)) \quad (1)$$

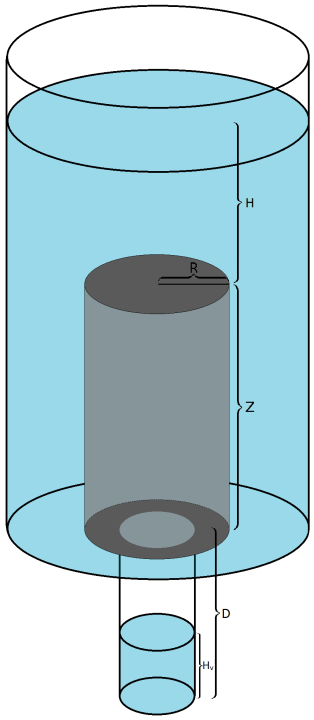

Figure 1: Sample

where the saturation θ, depending on pressure head h, is of the form

$$\theta(h) = \theta_r + (\theta_s - \theta_r)\theta_{ef}(h), \tag{2}$$

with irreducible saturation θ_r, porosity θ_s and effective saturation $\theta_{ef}(h)$.

We consider the fundamental saturation-pressure law in terms of van Genuchten-Mualem empirical model $h \leq 0$ in unsaturated zone

$$\theta_{ef}(h) = \frac{1}{(1 + (\alpha h)^n)^{\frac{1}{m}}}, \tag{3}$$

where $\alpha,\ n,\ m = 1 - \frac{1}{n}$ are soil parameters. In saturated zone we have $\theta_{ef} = 1$, $h > 0$.

The hydraulic permeability $K = K(h)$ is in van Genuchten-Mualem model

$$K(h) = K_s\,(\theta_{ef}(h))^{\frac{1}{2}} \cdot \left(1 - (1 - (\theta_{ef}(h))^m)^{\frac{1}{m}}\right)^2, \tag{4}$$

where K_s (also soil parameter) is a hydraulic permeability for saturated porous media, i.e., $K_s = K(0)$.

The flux in cylindrical coordinates is of the form

$$\mathbf{q} = -(q^r, q^z)^T, \tag{5}$$

$$q^r = K(h)\partial_r h,\ q^z = K(h)(\partial_z h - \beta).$$

The flow model is expressed in the form of Richard's equation

$$\partial_t \theta(h) = \frac{1}{r}\partial_r(rK(h)\partial_r h) + \partial_z(K(h)(\partial_z h - 1)). \tag{6}$$

We note that our model includes both saturated (elliptic partial differential equation) and unsaturated (parabolic partial differential equation) zones. We consider initially (at $t = 0$) the dry sample $h = -\infty$), but in the numerical experiments we use $h = -200$.

The top of our sample $\Gamma_{top} = \{r \in (0, R), z = Z\}$ is isolated, i.e., we consider $q_z = 0$ and the same condition we consider on the part $\{r \in (R1, R), z = 0\}$ of the bottom. Through the part $\Gamma_{out} = \{r \in (0, R1), z = 0\}$ the infiltrated water can outflow to the collection chamber, i.e. we consider $\partial_z h = 0$ on Γ_{out} in q^z (see (5)). The boundary condition on the sample mantel $\Gamma_{mant} = \{r = R, z \in (0, Z)\}$ reflects the hydrostatic pressure generated by water level $H(t) \geq 0$ (measured from the top of the sample) at the coordinate $0 \leq z \leq Z$. Then our boundary condition on Γ_{mant} is

$$h(t, R, z) = H(t) + (Z - z). \tag{7}$$

Due to the mass balance argument, the change in $H(t)$ reflects the infiltration flux through Γ_{mant} for $t > 0$. Thus, our system is closed by ODE

$$\dot{H}(t) = -Q \int_{\Gamma_{mant}} q^z\, d\Gamma_{mant}, \tag{8}$$

where Q is the ratio of the areas of Γ_{top} and the cross-section of inflow chamber. The amount of outflow water in the collection chamber is given by

$$M_{out}(t) = \int_0^t \int_{\Gamma_{out}} q^z\, d\Gamma_{out})dt,$$

which could be expressed in terms of water level

$$H_{out}(t) = Q_1 M_{out}(t),$$

where Q_1 is the ratio of areas Γ_{out} of the cross-section area and collection area of the collection chamber.

Conservation of contamination in water is expressed (in Cartesian coordinates) in partial differential equation.

2.2 Contaminant transport in the water

Denote by w the concentration of a contaminant dissolved in the water. Its transportation in porous media is governed by water flux $\mathbf{q}$, molecular diffusion

D_o and dispersion characterized in cylindrical coordinates by the matrix

$$\bar{D} = \begin{pmatrix} D_{1,1} & D_{1,2} \\ D_{2,1} & D_{2,2} \end{pmatrix} = \begin{pmatrix} \alpha_L (q^r)^2 + \alpha_T ((q^z)^2 & (\alpha_L - \alpha_T)(q^r q^z) \\ (\alpha_L - \alpha_T)(q^r q^z) & \alpha_L (q^z)^2 + \alpha_T (q^r)^2 \end{pmatrix} \frac{1}{|\vec{q}|}, \tag{9}$$

where α_L is longitudinal coefficient and α_T is transversal coefficient.

Denote by Qw contaminant flux,

$$Qw^r = -q_r w + \theta(D_{1,1}\partial_r w + D_{1,2}\partial_z w + D_o\theta \tag{10}$$

$$Qw^z = -q_z T w + \theta(D_{2,1}\partial_r w + D_{2,2}\partial_z w + D_o\theta. \tag{11}$$

Then, our mathematical model for contaminant transport with adsorption (in cylindrical coordinates) reads

$$\partial_t(\theta w) - \left(\frac{1}{r}\partial_r(rQw^r) + \partial_z(Qw^z\right) = -\rho\partial_t S. \tag{12}$$

2.3 Adsorption

The adsorption kinetic is governed by the ODE

$$\partial_t S = \kappa(\Psi(w) - S), \tag{13}$$

where S represents the adsorbed contaminant by a unit mass of porous media. Here, κ is the adsorption rate coefficient and describes the velocity of adsorption. The mathematical model (13) is a very special one and all the results obtained here can be easily extended to other models. The most common isotherms are $\Psi(s) = as$ (linear); $\Psi(s) = as^b$ (Freundlich); $\Psi(s) = \frac{as}{1+bs}$ (Langmuir); $\Psi(s) = \frac{as^r}{1+bs^r}$ (Mixed Freundlich-Langmuir).

2.4 Boundary Conditions

The governing equations are completed by a corresponding boundary and initial conditions. For simplicity we assume that on the boundary the contaminant concentration is constant W_0 and the contaminant is transported by water flow through the mantel $\Gamma_{mant} = \{r = R, z \in (0, Z)\}$ only. On the sample bottom part $\Gamma_{out} = \{r \in (0, R1), z = 0\}$ is a cumulated water outflow

$$M_{out}(t) = \int_0^t \int_{\Gamma_{out}} q^z \, d\Gamma_{out})dt$$

with the cumulated contaminant outflow

$$MW_{out}(t) = \int_0^t \int_{\Gamma_{out}} q^z \, w d\Gamma_{out})dt.$$

In solving inverse problems we shall assume the measurements of the time evolution of concentration of cumulated water outflow OM,

$$OM(t) = \frac{MW_{out}(t)}{M_{out}(t)}.$$

In our numerical experiments we assume the following model data:
$\theta_0 = 0.38$, $\theta_r = 0$, $K_s = 2.4\ 10^{-4}$, $\alpha = 0.0189$, $n = 2.81$, $g = 981$, $\alpha_L = 1$, $\alpha_T = \frac{1}{8}$, $\rho = 1$ and $\kappa = 0.05$, $h = -200$, $W_0 = 1, S_0 = 0$.

We consider the Langmuir adsorption isotherm with the coefficients $a = 2, b = 1$. We present the solution in the following three experiments scenarios, where the flow boundary conditions are presented before and the initial conditions will be specified in experiments.

In experiment 1 the infiltrated water concentration is $w = 1$. The initial sample saturation is almost zero, $h = -200$ and $S_0 = 0$, $t \in (0, 1500)$.

In experiment 2 the boundary and initial conditions are the same in $t \in (0, 200)$. For $t \in (200, 1500)$ the infiltrating water has concentration $w = 0$.

In experiment 3 we assume $S_0 = 0,5$ and the concentration of infiltrated water $w = 0$ for $t \in (0, 1500)$.

3 Numerical realization

We apply in our approximation scheme a flexible time stepping and a finite volume method in space variables.

We consider uniform partition of the domain in numerical experiments with $(N_x, N_y) = (31, 31)$ grid points $(r_i, z_j) = (i\Delta r, j\Delta z)$, $i, j = 0, 1, ..., 30$, $\Delta r = \frac{X}{N_r - 1}, \Delta z = \frac{Y}{N_z - 1}$.

We approximate the time derivative by backwards difference and then we integrate our system over the angular control volume $V_{i,j}$ with the corners $r_{i\pm1/2}, z_{j\pm1/2}$ and with the length $(\Delta r, \Delta z)$ of the edges. Then, our approximation linked with the inner grid point (r_i, z_j) at the time $t = t_k$ is followed.

$$\begin{aligned} &\frac{\theta(h) - \theta(h^{k-1})}{\tau}\Delta r\Delta z \\ &- \Delta z \frac{r_{i+1/2}}{r_i}\left[\frac{K(h_{i+1}) + K(h)}{2}\left(\frac{h_{i+1} - h}{\Delta r}\right)\right] \\ &+ \Delta z \frac{r_{i-1/2}}{r_i}\left[\frac{K(h) + K(h_{i-1})}{2}\left(\frac{h - h_{i-1}}{\Delta r}\right)\right] \\ &- \Delta r\left[\frac{K(h_{j+1}) + K(h)}{2}\left(\frac{h_{j+1} - h}{\Delta z} - 1\right)\right] \\ &+ \Delta r\left[\frac{K(h) + K(h_{j-1})}{2}\left(\frac{h - h_{j-1}}{\Delta z} - 1\right)\right] = 0 \end{aligned} \tag{14}$$

3.1 Quasi-Newton linearisation

In each (r_i, z_j) we linearise θ in terms of h iteratively (with iteration parameter l) following [Celia et al.,] in the following way

$$\frac{\theta(h^{k,l+1}) - \theta(h^{k-1})}{\tau} = C^{k,l}\frac{h^{k,l+1} - h^{k,l}}{\tau} + \frac{\theta^{k,l} - \theta^{k-1}}{\tau},$$

where

$$C^{k,l} = \frac{\partial \theta^{k,l}}{\partial h^{k,l}} =$$
$$(\theta_s - \theta_r)(1-n)\alpha(\alpha h^{k,l})^{n-1}(1 + (\alpha h^{k,l})^n)^{-(m+1)}$$

for $h^{k,l} < 0$, else $C^{k,l} = 0$. We stop iterations for $l = l^*$, when $h^{k,l^{*+1}} - h^{k,l^*} < \varepsilon$ and then we put $h^k := h^{k,l^*+1}$. Finally we replace the non-linear term $K(h^k)$ by $K(h^{k,l})$, and our approximation scheme became linear in terms of $h^{k,l+1}$.

Generally, we speed the iteration by a special construction of starting point $h^{k,0} \approx h^{k-1}$ and using suitable damping parameter in solving corresponding linearised system. Solution of complex system by operator splitting method. To obtain approximate solution for contaminant in water and matrix at the time section $t = t_k$ when starting from $t = t_{k-1}$ we use the obtained flow characteristics from $t = t_k$ for θ^k, h^k and $\vec{q}^k$ and for matrix $\bar{D}^k$.

3.2 Approximation scheme for contaminant

For w at (r_i, z_j) for $t = t_k$ we obtain by finite volume

$$\begin{aligned}
&\theta\frac{w - w^{k-1}}{\tau}\Delta r\Delta z \\
&- \Delta z\left[\frac{1}{r_i}(r_{i+1/2}Qw^r_{i+1/2} - r_{i-1/2}Qw^r_{i-1/2})\right] \\
&+ \Delta r\left[Qw^z_{j+1/2} - Qw^z_{j-1/2})\right] \\
&= -\Delta r\Delta z\rho\psi(w^{k-1}) - S^{k-1}),
\end{aligned}$$

where $\partial_z w$ in Qw^r in the point $\{r_{i+1/2}, z_j\}$ is approximated by

$$\frac{w_{i+1,j+1} + w_{i,j+1} - w_{i+1,j-1} - w_{i,j-1}}{4\Delta z}$$

and in the point $\{r_{i-1/2}, z_j\}$ we shift i by $i-1$. Analogously we approximate $\partial_r w$ in Qw^z, where the role of indexes i and j is interchanged. Finally, we have to approximate the items in the dispersion matrix D arising in Qw^r, Qw^z.

We approximate K, $\vec{q}$ and D in middle points by

$$\begin{aligned}
K_{i\pm\frac{1}{2}} &= \frac{K(h_{i\pm1}) + K(h_i)}{2} \\
K_{j\pm\frac{1}{2}} &= \frac{K(h_{j\pm1}) + K(h_j)}{2} \\
q^r_{i\pm\frac{1}{2}} &= -K_{i\pm\frac{1}{2}}\left(\frac{\pm h_{i\pm1} \mp h_i}{\Delta r}\right) \\
q^z_{j\pm\frac{1}{2}} &= -K_{j\pm\frac{1}{2}}\left(\frac{\pm h_{j\pm1} \mp h_j}{\Delta z} - 1\right) \\
q^z_{i\pm\frac{1}{2}} &= -K_{i\pm\frac{1}{2}}\left(\frac{h_{i\pm1,j+1} + h_{i,j+1} - h_{i\pm1,j-1} - h_{i,j-1}}{4\Delta z} - 1\right) \\
q^r_{j\pm\frac{1}{2}} &= -K_{j\pm\frac{1}{2}}\left(\frac{h_{i+1,j\pm1} + h_{i+1,j} - h_{i-1,j\pm1} - h_{i-1,j}}{4\Delta r}\right) \\
D_{1,1,i\pm\frac{1}{2}} &= \frac{\alpha_L(q^r_{i\pm\frac{1}{2}})^2 + \alpha_T(q^z_{i\pm\frac{1}{2}})^2}{\sqrt{(q^r_{i\pm\frac{1}{2}})^2 + (q^z_{i\pm\frac{1}{2}})^2}} + \lambda\theta_{i\pm\frac{1}{2}} \\
D_{1,2,i\pm\frac{1}{2}} &= \frac{(\alpha_L - \alpha_T)q^r_{i\pm\frac{1}{2}}q^z_{i\pm\frac{1}{2}}}{\sqrt{(q^r_{i\pm\frac{1}{2}})^2 + (q^z_{i\pm\frac{1}{2}})^2}}
\end{aligned}$$

$$D_{2,2,j\pm\frac{1}{2}} = D_{1,1,i\pm\frac{1}{2}}\ (i \leftrightarrow j; \alpha_L \leftrightarrow \alpha_T)$$
$$D_{2,1,j\pm\frac{1}{2}} = D_{1,2,i\pm\frac{1}{2}}\ (i \leftrightarrow j).$$

3.3 Approximation scheme for adsorption

We apply the same finite volume method and in the point (r_i, z_j) at $t = t_k$ we obtain

$$\frac{S^k - S^{k-1}}{\tau}\Delta r\Delta z = \Delta r\Delta z\kappa(\psi(w^k) - S^{k-1}).$$

To obtain approximation linked with the boundary points we apply the same strategy of finite volume method where the control volume $V_{i,j}$ is only half or quoter of the $\Delta r\Delta z$ corresponding to the inner grid points.

4 Numerical experiments

4.1 Inverse problem: determination of κ, ψ

Measuring the concentration of cumulated outflow water $OM(t)$ will be the main information source of adsorption mechanism. We propose the infiltration scenarios, described by boundary and initial conditions before, which enable us to measure (κ, ψ).

We will focus to Langmuir adsorption isotherm, where except of κ we have to determine the coefficients $\{a, b\}$. We assume the time interval $(0, 1500)$ with 31 uniformly distributed time moments $\{t_i\}_1^{31}$, where we expect measurements of $OM(t_i)$. On the

other hand, we solve our system with some given parameters $p = \{a, b, \kappa\}$ and obtain $OM_c(t_i)$. Solution of our inverse problem consists in determination of p which minimizes the $||\{OM(t_i) - OM_c(t_i)\}_1^{31}||$. This could be realized iteratively using some minimization software. We use "fminsearch" from Matlab toolbox.

We test the practical applicability of our suggested experiment scenario with efficiency of our numerical method in the following way. We compute OM_c using same "standard" model parameter p_s, e.g., $p_s = \{2, 1, 0.05\}$. Then we "forget " p_s and instead we use a starting parameter p_o in minimization procedure. The optimal solution p_{opt} (with respect to some "tolerance") we compare with our model parameter p_s. Stability and reliability of our method we verify in series of experiments, where dependence on the choice of starting parameters and the level of noise applied to OM_c is taken into account.

The convergence of minimization procedure is strongly linked with expected local minima, which we test with the change of starting parameters. To increase the reliability of p_{opt} we can extend the measurements vector $OM_c \equiv OM_c^{(I)}$ to $\{OM_c^{(I)}, OM_c^{(II)}, OM_c^{(III)}\}$ linked with the solution of Experiments I-III described before.

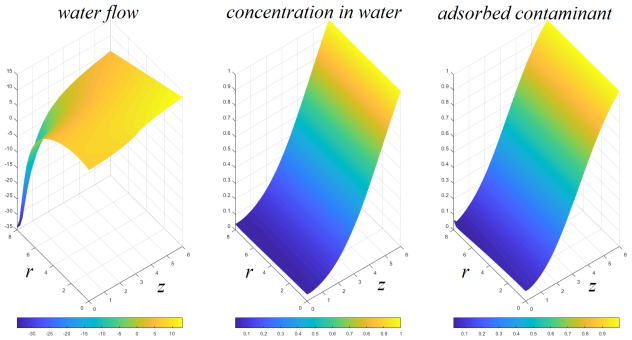

Figure 2: Water pressure h, concentration in water w and adsorbed contaminant S in time $t = 330$ in experiment 1

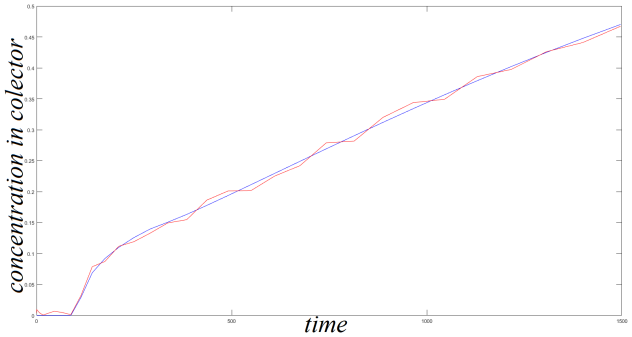

Figure 3: Time evolution of concentration of cumulated outflow water in experiment 1

4.2 Results in experiment 1

In the experiment 1 we can see, that contaminant in water is infiltrating together with water very quickly, because of negative pressure h. Therefore the concentration of the outflow water is increasing fast. After 350 seconds the cylinder is fully saturated, so water flow slows down rapidly and contaminant is adsorbed into the sample. Because of that, concentration of the water in the collection chamber is increased slower as we can see in figure 3.

Determination of adsorption coefficients is relatively stable. We obtain error up to 8% with different noises up to 0.01 and with various starting points as we can see in table 1.

Table 1: Optimal values of a, b, κ for $p_s = [2, 1, 0.05]$ with noise 0.01 in experiment 1

p_{start}	p_{opt}
$[1, 0.5, 0.01]$	$[1.9901, 0.9484, 0.04934]$
$[1, 0.5, 0.01]$	$[1.9319, 0.9398, 0.05069]$
$[3, 0.5, 0.01]$	$[2.0059, 1.0529, 0.05099]$
$[3, 0.5, 0.01]$	$[2.0774, 1.0515, 0.04929]$
$[1, 2, 0.01]$	$[1.9904, 1.0384, 0.05024]$
$[1, 2, 0.01]$	$[1.9943, 0.9523, 0.04971]$
$[3, 2, 0.01]$	$[2.0555, 1.0427, 0.04930]$
$[3, 2, 0.01]$	$[1.9226, 1.0558, 0.04976]$
$[1, 0.5, 0.1]$	$[1.9303, 1.0381, 0.05010]$
$[1, 0.5, 0.1]$	$[1.9190, 1.0596, 0.04943]$
$[3, 0.5, 0.1]$	$[1.9801, 0.9355, 0.04907]$
$[3, 0.5, 0.1]$	$[1.9697, 1.0707, 0.04982]$
$[1, 2, 0.1]$	$[1.9493, 1.0306, 0.05079]$
$[1, 2, 0.1]$	$[1.9372, 1.0650, 0.05028]$
$[3, 2, 0.1]$	$[1.9214, 0.9552, 0.04981]$
$[3, 2, 0.1]$	$[2.0414, 1.0373, 0.04969]$

4.3 Results in experiment 2

In this experiment, contaminated water is infiltrating 180 seconds. Part of the cylinder is still almost dry, when we change the boundary condition, where water with zero concentration is infiltrated. We can see, that contaminant is adsorbed into the sample and concentration in outflow chamber is increasing, but after that, uncontaminated water causes desorption in the sample. It causes decreasing of concentration in outflow chamber as we can see in figure 5.

This method is very stable. As we can see in table 2, error of the adsorption coefficients is up to 5% with different noises up to 0.01 and with various starting points.

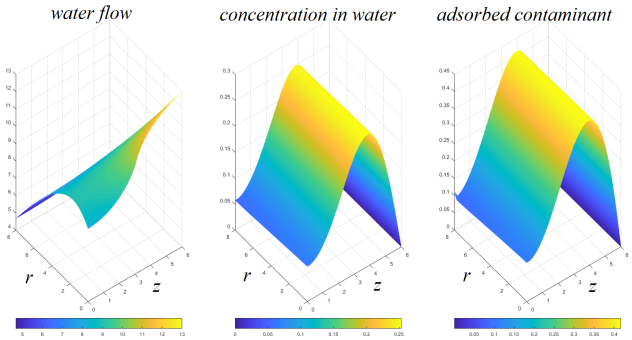

Figure 4: Water pressure h, concentration in water w and adsorbed contaminant S in time $t = 350$ in experiment 2

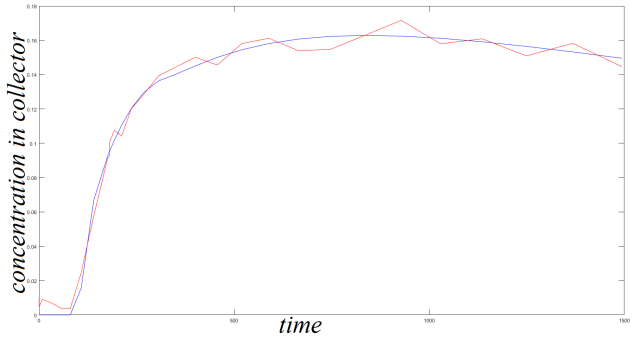

Figure 5: Time evolution of concentration of cumulated outflow water in experiment 2

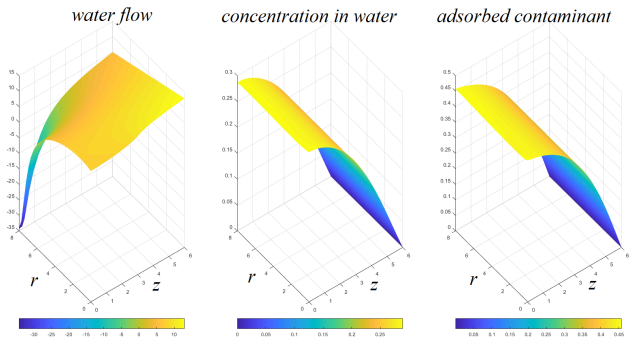

Figure 6: Water pressure h, concentration in water w and adsorbed contaminant S in time $t = 330$ in experiment 3

Table 2: Optimal values of a, b, κ for $p_s = [2, 1, 0.05]$ with noise 0.01 in experiment 2

p_{start}	p_{opt}
$[1, 0.5, 0.01]$	$[1.9604, 0.9852, 0.04912]$
$[1, 0.5, 0.01]$	$[2.0242, 0.9655, 0.05033]$
$[3, 0.5, 0.01]$	$[2.0790, 1.0039, 0.05058]$
$[3, 0.5, 0.01]$	$[2.0533, 1.0242, 0.04961]$
$[1, 2, 0.01]$	$[2.0313, 1.0339, 0.05042]$
$[1, 2, 0.01]$	$[1.9407, 1.0353, 0.05039]$
$[3, 2, 0.01]$	$[2.0444, 0.9768, 0.04936]$
$[3, 2, 0.01]$	$[1.9124, 1.0131, 0.05055]$
$[1, 0.5, 0.1]$	$[2.0227, 1.0328, 0.05040]$
$[1, 0.5, 0.1]$	$[1.9208, 1.0081, 0.05056]$
$[3, 0.5, 0.1]$	$[1.9076, 1.0047, 0.05011]$
$[3, 0.5, 0.1]$	$[2.0311, 0.9689, 0.04935]$
$[1, 2, 0.1]$	$[1.9283, 0.9673, 0.04965]$
$[1, 2, 0.1]$	$[2.0323, 1.0222, 0.04950]$
$[3, 2, 0.1]$	$[1.9331, 1.0388, 0.05038]$
$[3, 2, 0.1]$	$[1.9073, 0.9531, 0.04962]$

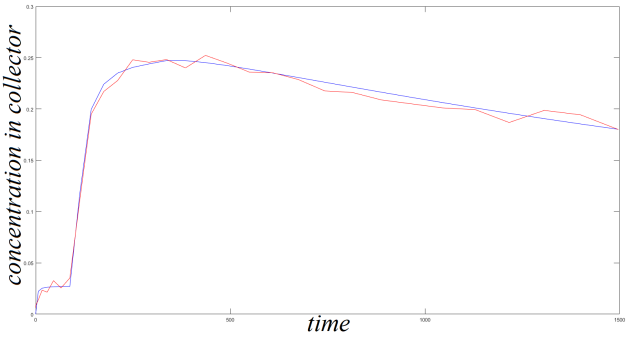

Figure 7: Time evolution of concentration of cumulated outflow water in experiment 3

4.4 Results in experiment 3

In experiment 3 we assume $S_0 = 0,5$ and infiltrated water has concentration $w = 0$. Therefore desorption happens. When the sharp front of infiltrated water reaches Γ_{out}, concentration of the water in the collection chamber increases rapidly, because of the desorption. The adsorbed contaminant in sample is decreasing and therefore concentration of the water in outflow chamber is decreasing too as we can see in figure 7.

This experiment is not very stable for determination of adsorption coefficients, because it is very sensitive for measured data. We obtained error up to 15% with different noises up to $0,01$ as we can see in table 3.

Table 3: Optimal values of a, b, κ for $p_s = [2, 1, 0.05]$ with noise 0.01 in experiment 3

p_{start}	p_{opt}
$[1, 0.5, 0.01]$	$[1.8492, 1.1096, 0.05065]$
$[1, 0.5, 0.01]$	$[2.1265, 0.8877, 0.05052]$
$[3, 0.5, 0.01]$	$[2.2637, 0.9220, 0.04833]$
$[3, 0.5, 0.01]$	$[2.2856, 0.9014, 0.04709]$
$[1, 2, 0.01]$	$[2.0028, 1.0397, 0.05193]$
$[1, 2, 0.01]$	$[2.2791, 0.9812, 0.05074]$
$[3, 2, 0.01]$	$[1.7800, 0.9144, 0.04766]$
$[3, 2, 0.01]$	$[1.7770, 1.0251, 0.05200]$
$[1, 0.5, 0.1]$	$[1.9064, 1.1218, 0.04914]$
$[1, 0.5, 0.1]$	$[1.8867, 1.0865, 0.04929]$
$[3, 0.5, 0.1]$	$[1.9636, 1.1481, 0.05132]$
$[3, 0.5, 0.1]$	$[1.7279, 0.9413, 0.04992]$
$[1, 2, 0.1]$	$[1.8213, 1.0419, 0.05116]$
$[1, 2, 0.1]$	$[1.9776, 1.0960, 0.04753]$
$[3, 2, 0.1]$	$[2.1859, 1.0165, 0.04844]$
$[3, 2, 0.1]$	$[1.7631, 0.9642, 0.05070]$

5 Conclusion

Numerical experiments demonstrate efficiency of our numerical method also in more dimensional case using only non-invasive measurements. The $0,01$ noise in our measurements effects the $5 - 8\%$ defect with three adsorption coefficients in experiments 1 and 2. In the experiment 3 the defect reaches up to 15%. During series of experiments we have remarked very low dependence of optimal solution on starting points. Greater dependence is linked to the type of generated noise.

We developed efficient numerical method for determination of adsorption coefficients on the base of finite volume method. Operator splitting method is used to solve an complex system for water infiltration, contaminant transport by water including the adsorption with the matrix.

The 3D experimental scenario significantly decrease the influence of preferential streamlines appearing in 1D laboratory experiments (with thin tubes).

Acknowledgements: The authors confirm a support by the Slovak Research and Development Agency APVV-15-0681 and VEGA 1/0565/16.

References:

[Bear and Cheng, 2010] Bear, J. and Cheng, A. H.-D. (2010). Modeling groundwater flow and contaminant transport. *Springer*, 23.

[Bergman et al., 2011] Bergman, T. L., Lavine, A. S., Incropera, F. P., and DeWitt, D. P. (2011). *Fundamentals of Heat and Mass Transfer*. John Wiley and Sons, 7th edition.

[Celia et al.,] Celia, M. A., Bouloutas, E. T., and Zarba, R. L. A general mass conservative numerical solution for the unsaturated flow equation. *Water Resources Research*, 26(7):1483–1496.

[Constales and Kačur, 2001] Constales, D. and Kačur, J. (2001). Determination of soil parameters via the solution of inverse problems in infiltration. *Computational Geosciences*, 5(1):25–46.

[Kačur et al., 2016] Kačur, J., Mihala, P., and Tóth, M. (2016). Determination of soil parameters under gravitation and centrifugal forces in 3d infiltration. *WSEAS TRANSACTIONS on HEAT and MASS TRANSFER*, 11:115–120.

[Kačur and Minar, 2013] Kačur, J. and Minar, J. (2013). A benchmark solution for infiltration and adsorption of polluted water into unsaturated saturated porous media, a solution for infiltration and adsorption. *Transport in porous media*, 97.

[Simunek et al., 2008] Simunek, Jiri, J., Saito, H., Sakai, M., and Van Genuchten, M. (2008). *The HYDRUS-1D Software Package for Simulating the One-Dimensional Movement of Water, Heat, and Multiple Solutes in Variably-Saturated Media*.